

See discussions, stats, and author profiles for this publication at: <https://www.researchgate.net/publication/282012566>

UV-controlled Shape Memory Hydrogels Triggered By Photoacid Generator

ARTICLE *in* RSC ADVANCES · SEPTEMBER 2015

Impact Factor: 3.84 · DOI: 10.1039/C5RA14421C

READS

13

6 AUTHORS, INCLUDING:



Wei Feng

University of Science and Technology of Ch...

3 PUBLICATIONS 6 CITATIONS

SEE PROFILE

COMMUNICATION

CrossMark
click for updatesCite this: *RSC Adv.*, 2015, 5, 81784

Received 21st July 2015

Accepted 22nd September 2015

DOI: 10.1039/c5ra14421c

www.rsc.org/advances

UV-controlled shape memory hydrogels triggered by photoacid generator†

Wei Feng,^a Wanfu Zhou,^b Shidong Zhang,^b Yujiao Fan,^a Akram Yasin^a
and Haiyang Yang^{*a}

Light-induced shape memory polymers represent a class of stimuli-responsive materials that can recover their permanent shapes from temporarily trapped ones upon exposure to light illumination. Although much effort has been devoted to developing various light-responsive shape memory polymers, fabrication of such a light-responsive shape memory hydrogel still remains a challenge compared to neat polymers in their dry state. Herein, we developed a facile and general strategy to endow conventional hydrogel systems with ultraviolet (UV)-controlled shape memory performance simply using a photoacid generator (PAG) as a trigger. The process involves shape fixity through coordination interaction between imidazole groups and metal ions, and shape recovery by switching off the complexation *via* PAG photolysis reaction which leads to the protonation of imidazole groups. Furthermore, this convenient strategy is proved to be applicable to other pre-existing hydrogels such as a boronate ester cross-linked melamine–poly(vinyl alcohol) (PVA) hydrogel. We believe this method could provide a new opportunity with regard to the design and practical application of light-controlled shape memory hydrogels.

Light-responsive shape memory polymers (SMPs) have attracted increasing attention mainly due to the distinct features of light such as remotely, spatially, and easily controlled “on-off” activation.^{1–3} Light-responsive shape memory bulk polymer composites are commonly based on photo-cross-linking/isomerization reaction,^{4–6} or photothermal effects.^{1,7–11} For example, photochromic moieties such as coumaric acid or cinnamylidene acetic acid, undergo desired reversible photo-cross-linking reaction upon absorption of photons and afford additional network to fix a temporary shape. *Trans–cis*

photoisomerization of azobenzene groups could be employed to achieve anisotropic bending of polymer films in response to light.⁶ Photothermal shape memory property was obtained when photothermal effect fillers (e.g. gold nanoparticle,^{8,10,12} gold nanorod,¹³ carbon nanotube,⁷ dye/ligand,^{11,14} and graphene^{15–17}) were introduced into a polymer matrix bearing thermo-sensitive microdomain structures.

However, when it comes to fabrication of a light-controlled shape memory hydrogel, the strategies above-mentioned for neat polymer in their dry state are not suitable. The main confinement is mainly attributed to the low solubility of the photochromic moieties and similar organic functional groups in water. Analogously, the hydrophobic nature of photothermal gradients makes them prone to aggregation in water without functionalization strategies.^{11,12,16} Thus, photo-responsive shape memory hydrogels have been rarely reported.

Previously, we reported chemically or thermally activated shape memory hydrogels bearing ligand-Fe³⁺ complexation^{18,19} or crystalline domains,²⁰ respectively. Herein, we develop a facile and general Photoacid Generator strategy to endow different hydrogel systems with light-controlled shape memory performance simply using photoacid generator (PAG) as a trigger. For instance, as shown in Fig. 1, after treated with a mixture solution of metal ions (Cu²⁺, Zn²⁺, or Ni²⁺) and PAG (diphenyliodonium nitrate), an organic cross-linked poly(acrylamide-*co*-*N*-vinylimidazole) hydrogel is trapped in a temporary state because of a drastic enhancement of mechanical strength resulted from coordination interaction between metal ions and imidazole groups. Upon UV irradiation, PAG is photolyzed to generate protons to lower the pH below the pK_a (~5.8) of imidazole groups, leading to disassociation of the complexation effect. Consequently, the temporary shape recovers its permanent form which is determined by organic cross-linkers. This simple method, where PAG plays a critical role, is also applicable to other conventional systems such as a boronate ester cross-linked melamine–poly(vinyl alcohol) (PVA) physical network. Thus, we hope that this facile strategy may

^aCAS Key Laboratory of Soft Matter Chemistry, Department of Polymer Science and Engineering, University of Science and Technology of China, Hefei, Anhui 230026, P. R. China. E-mail: yhy@ustc.edu.cn

^bOilfield Production Technology Institute, Daqing Oilfield Co. Ltd, Daqing 163514, P. R. China

† Electronic supplementary information (ESI) available. See DOI: 10.1039/c5ra14421c

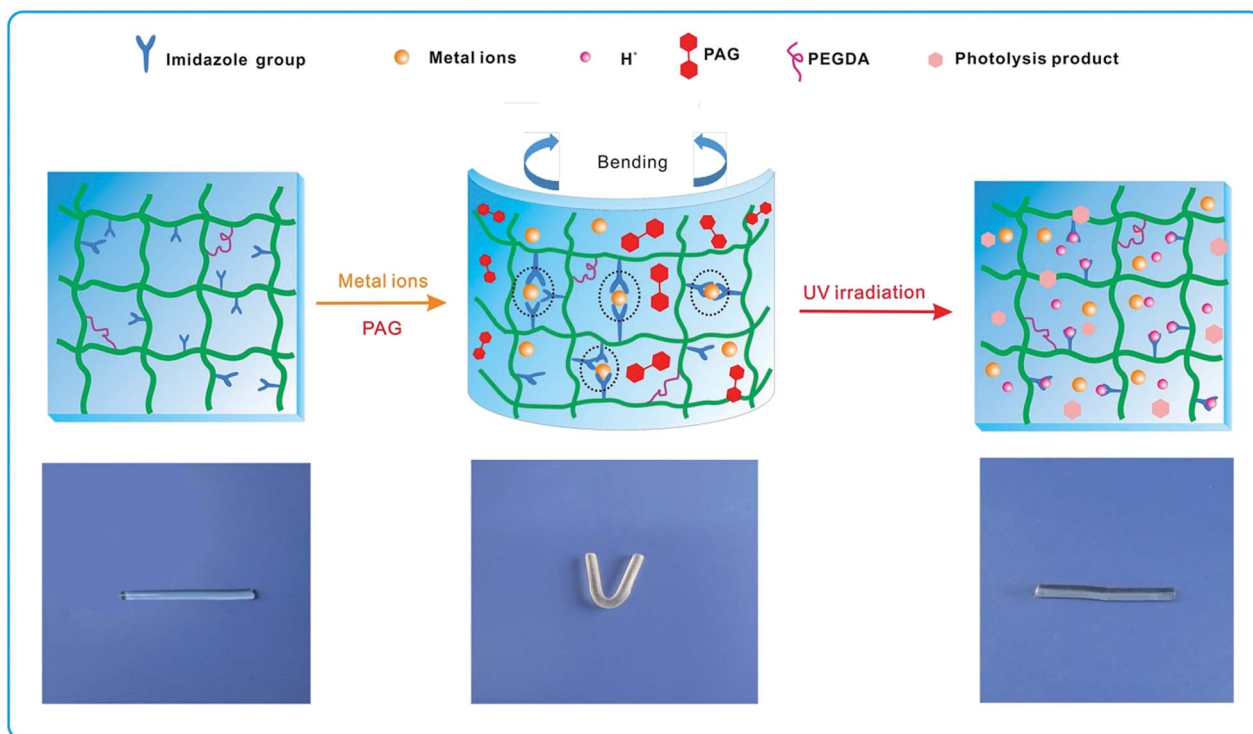


Fig. 1 Illustration of UV light-responsive shape memory hydrogel mechanism.

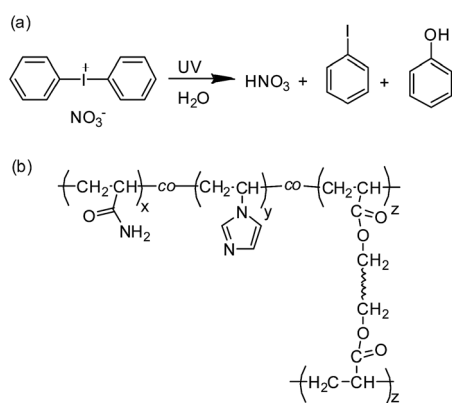
provide new opportunities for both designing and application of light-controlled shape memory hydrogels.

P(AM-co-VI) hydrogels were prepared through free radical polymerization. (Detailed synthesis procedure can be found in ESI†) Briefly, after preparing mixture solutions containing different amounts of acrylamide, *N*-vinylimidazole and cross-linker polyethylene glycol diacrylate (PEGDA), ammonium persulfate (initiator) and tetramethylethylenediamine (accelerator) were added to initiate the polymerization to obtain hydrogels with varied compositions.

The chemical structures of prepared hydrogels (Scheme 1) are confirmed by FTIR spectra. The FTIR spectra of samples

with different VI contents are listed in Fig. 2. The band at 1668 cm^{-1} is attributed to $\text{C}=\text{O}$ in acrylamide and PEGDA.^{21,22} Bands from imidazole groups are verified at 1500 cm^{-1} ($\text{C}=\text{C}$ and $\text{C}=\text{N}$ stretching vibrations), 1416 cm^{-1} (imidazole ring stretching vibrations), 1228 cm^{-1} (CH and $\text{C}-\text{N}$ in-plane bending) and 1083 cm^{-1} (CH in-plane bending and ring stretching). The strong band from $-\text{NH}_2$ group is verified, with stretching vibrations of $\text{N}-\text{H}$ at 3433 cm^{-1} . These characteristic peaks suggest successful synthesis of P(AM-co-VI) hydrogels.

Fig. 3a shows that the as-prepared hydrogels swelled in deionized water with water content (detailed swelling data can be found in Table S1, ESI†). Meanwhile, the swelling ratio increased with increasing acid concentration. The equilibrium



Scheme 1 (a) Photolysis reaction of photoacid generator PAG (diphenyliodonium nitrate); (b) chemical structure of P(AM-co-VI) hydrogel.

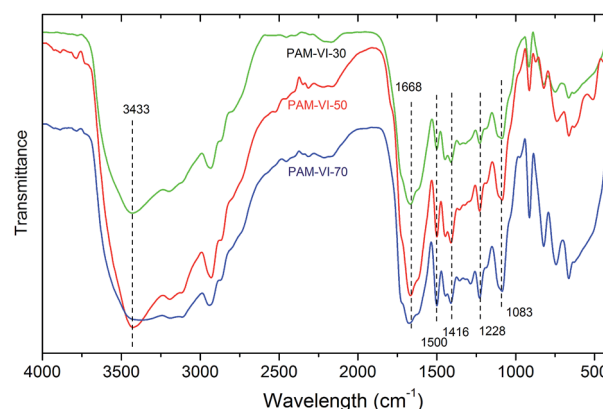


Fig. 2 FTIR spectra of samples with different VI/AM ratios.

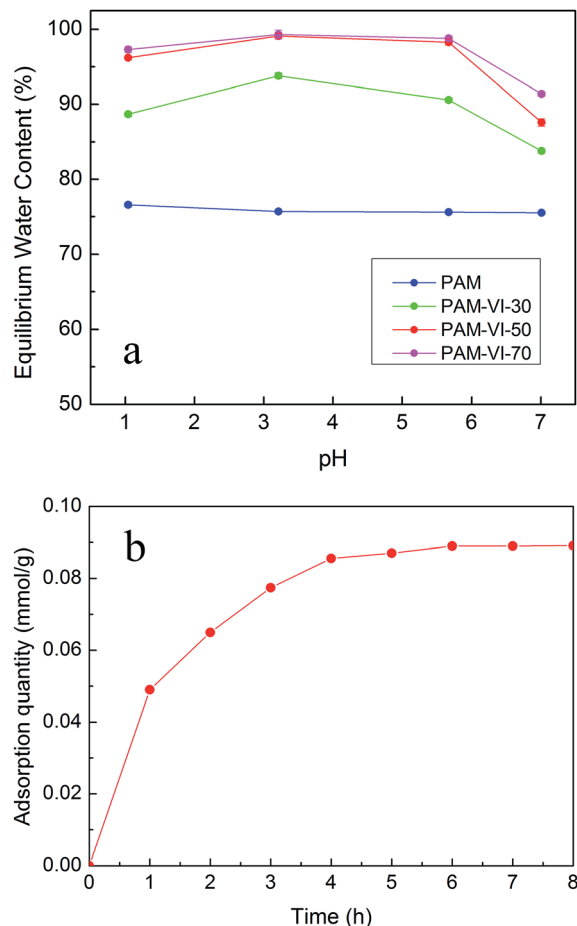


Fig. 3 (a) Swelling behaviour of hydrogels in water with different pH. (b) Adsorption kinetics of Zn^{2+} by PAM-VI-50 hydrogel from 10 mM ZnSO_4 solution.

water content (EWC) of PAM-VI-50 hydrogel increased from 60% to 87.6% in deionized water and increased from 87.6% at pH 7.01 to 99.1% at pH 3.21, and then decreased to 96.2% at pH 1.04. In the range $3.21 < \text{pH} < 7.01$, electrostatic repulsion between protonated imidazole groups causes increase in the swelling of hydrogels. And in the range $1.04 < \text{pH} < 3.21$, the decrease in the swelling ratio of hydrogels is attributed to the increasing ionic strength of the medium.^{23,24} Meanwhile, for the same pH, hydrogel with higher VI content exhibits higher EWC, which is attributed to the increasing repulsive electrostatic interaction between neighbouring protonated imidazole groups.²⁵

To study the adsorption kinetics of Zn^{2+} , atomic absorption spectroscopy assay was performed. Fig. 3b exhibits the adsorption kinetics of Zn^{2+} by PAM-VI-50 hydrogel in 10 mM ZnSO_4 solution. The adsorption of Zn^{2+} rises over time is revealed by corresponding decrease of Zn^{2+} concentration in the external solution. An absorption equilibrium is observed within 4 hours, implying that a maximum amount of Zn^{2+} is immobilized at the final state.

Fig. 4a depicts the effect of VI concentration on the mechanical strength of hydrogels. Decreasing the VI/AM molar

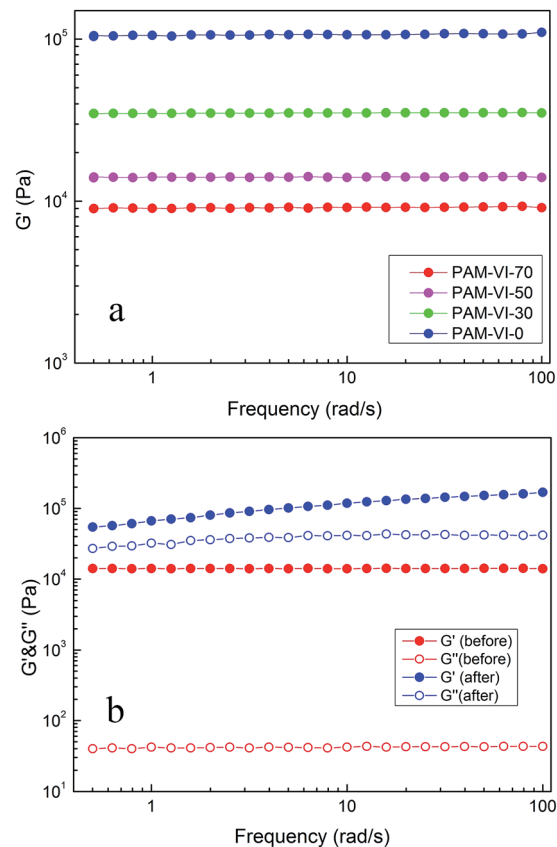


Fig. 4 (a) Storage moduli of different VA/AM ratios as a function of frequency. (b) Frequency sweep of PAM-VI-50 hydrogel before and after immersion in a mixture solution of ZnSO_4 (10 mM) and PAG (20 mM).

ratio leads to obvious increase of the G' values, revealing a relatively weaker network formed at a higher VI/AM ratio. It is reasonable that the hydrogel containing higher acrylamide content tends to exhibit stronger mechanical strength due to strong hydrogen bonding between amide groups, which serves as physical cross-linkages and contributes to denser polymeric network.^{26,27} In contrast, fewer hydrogen bonding points exist in the presence of higher VI/AM ratios.

Previous studies have confirmed that various metal ions can coordinate with imidazole groups and the stability constants of typically adopted metal ions are in the order: $\text{Cu}^{2+} > \text{Ni}^{2+} > \text{Zn}^{2+} > \text{Co}^{2+}$.^{28,29} In order to achieve desirable shape memory performance, the metal ions used here need to be selected delicately. Metal ion with relatively higher stability constant to imidazole group is appropriate for memorizing a temporary shape. Experiments show that binding affinity of imidazole groups to Cu^{2+} , Ni^{2+} , Zn^{2+} could provide sufficient strength to lock a temporary shape, whereas Co^{2+} is poorly efficient for shape memory. Taking into consideration the shape recovery, we choose Zn^{2+} as an example, with Cu^{2+} and Ni^{2+} as comparisons.

Fig. 4b shows the effect of ZnSO_4 -PAG on the mechanical properties of hydrogels. The G' values for as-prepared samples all exhibit substantial elastic response and are considerably larger than the G'' values over the entire range of frequencies,

indicative of predominantly elastic nature. After treated with ZnSO_4 -PAG, both the G' and G'' values display drastic enhancement. The increase of G' suggests that a stronger network is formed. Undoubtedly, reinforcement of the network is mainly attributed to strong coordination interaction between VI groups and Zn^{2+} . As another evidence of this, with the increase of VI/AM ratios, the gels show prominent increment in G' values. For instance, storage moduli of PAM-VI-70, PAM-VI-50 and PAM-VI-30 hydrogels increase to 37-fold, 12-fold and 1.38 fold (100 rad s^{-1}) of corresponding original values, respectively (Fig. S1, ESI†). Meanwhile, as a reference, the PAM hydrogel without VI exhibits a slightly higher G' , which could be attributed to ion-dipole interaction between Zn^{2+} ions and amide groups of polyacrylamide.^{30,31} It is worthwhile noting that slight frequency dependence shows up for the samples in the presence of Zn^{2+} ions compared to those as prepared ones, indicative of the existence of additional dynamic non-covalent interaction in hydrogels.

It is well-known that photoacid generator can undergo photolysis under UV irradiation.^{32–36} Here, we employ this facile method to endow hydrogel with shape memory ability. A straight strip gel with a length of 6 cm and radius of 4 mm was bent into a “V”-form shape and immersed in the solution containing ZnSO_4 (10 mM) and PAG (20 mM) for 4 hours to fix the temporary shape. Then it was subjected to UV irradiation with an Oriel 100 W mercury arc lamp to perform the shape recovery process. The hydrogels could be recycled for shape memory performance. Between cycles, to remove Zn^{2+} ions from the hydrogel, the used hydrogel was firstly soaked in 20 mM EDTA solution for three hours and then soaked in deionized water for two hours. The angle was recorded at certain time. According to previously published calculation methods,^{37–40} the shape fixity ratio R_f and shape recovery ratio R_r were defined by the following equations:

$$R_f = \frac{\Delta\theta_{u(N)}}{\Delta\theta_m} \times 100\%$$

$$R_r = \frac{\theta_{p(N)} - \theta_{u(N)}}{\theta_{p(N-1)} - \theta_{u(N)}} \times 100\%$$

where $\Delta\theta_m$ is the maximum angle change applied to the sample, $\Delta\theta_u$ is the fixed angle change reached after releasing external force. As depicted in Fig. S2 (ESI)†, θ_u stands for the “V” angle value in the end of fixity process, θ_p stands for the “V” angle value in the end of recovery process, and N represents the cycle number. In this definition, for an initial straight strip hydrogel, $\theta = 180^\circ$; for a curled “V”-shaped hydrogel, $\theta < 180^\circ$. As shown in Fig. 1, the strip gel is curled into a “V” shape under external stress and immersed in the mixture solution of ZnSO_4 and PAG (10 mM, 20 mM, respectively). Complexation between imidazole groups and Zn^{2+} enables the maintenance of the temporary shape. When subjected to UV irradiation, it regresses to the initial straight shape in 15 minutes. Organic cross-linker, polyethylene glycol diacrylate, is utilized to determine the permanent shape and prevent chain slippage. The recovery ratio accompanied by pH change over time is portrayed in Fig. 5a. Upon exposure to UV illumination, the pH value decreases

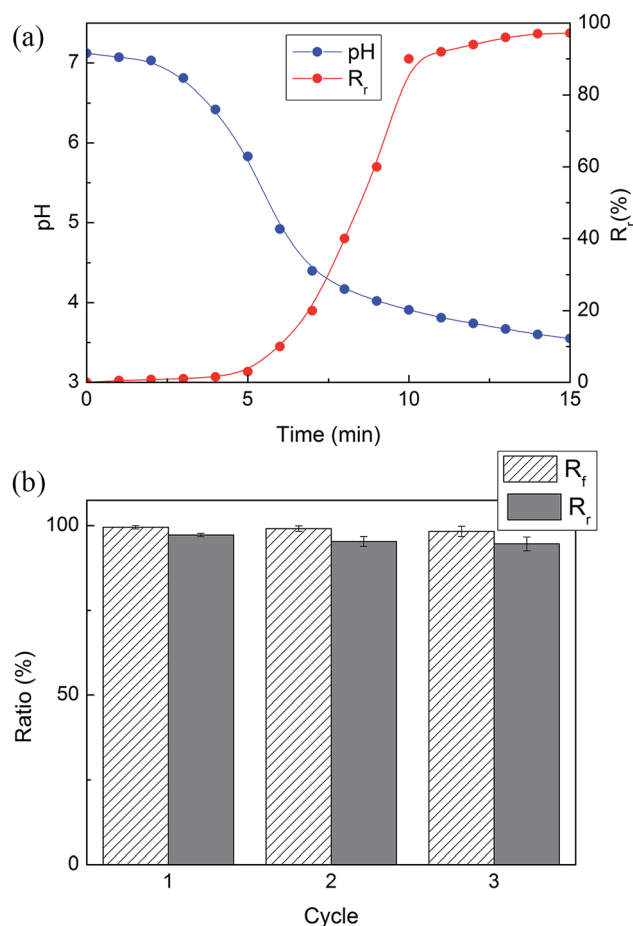


Fig. 5 (a) pH curve of 20 mM PAG solution and shape recovery ratio (R_r) as a function of UV irradiation time. (b) Cyclicity of PAM-VI-50 hydrogel shape memory process.

rapidly within several minutes, suggesting the production of protons from photolysis of diphenyliodonium nitrate. Meanwhile, the “V” shape gel begins to return to its permanent shape quickly. The complete recovery process finishes in 15 minutes with a final pH value around 3.7. Compared to those conventional pH-responsive or ion-extraction shape recovery systems, the present one possesses a much faster recovery capability.⁴¹ The cyclicity of shape memory process is evaluated by measuring shape fixity ratio (R_f) and shape recovery ratio (R_r) of three samples in three cycles. (Fig. 5b) The mechanical response also shows corresponding reversibility (Fig. S3, ESI†). In every cycle, the ZnSO_4 -PAG solution is freshly prepared and there are enough Zn^{2+} ions to form complexation with imidazole groups to enhance hydrogel's mechanical strength and lock its temporary shape. So R_f is quite stable during three cycles. The samples show compromised shape recovery ability with increasing cycle number, which can be attributed to the remaining Zn^{2+} ions in the hydrogel,¹⁹ slightly enhancing the mechanical strength of hydrogel (as shown in Fig. 6a, the hydrogel treated with UV light has a slightly higher G' than pristine hydrogel), preventing the hydrogel fully returning to its original shape.

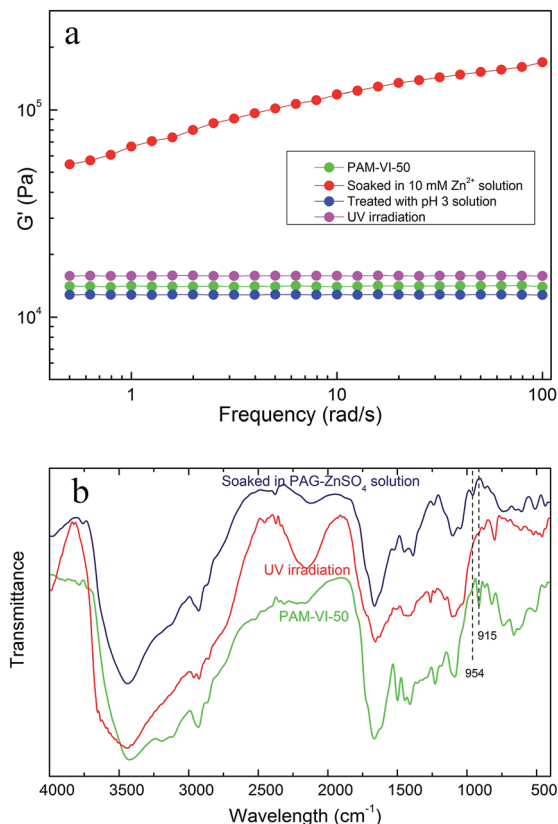


Fig. 6 (a) Storage moduli of (1) pristine PAM-VI-70 hydrogel, (2) hydrogel after immersed in 10 mM Zn^{2+} and 20 mM PAG solution for 4 hours, then hydrogel subjected to (3) UV light for 15 minutes, (4) pH 3 solution for 15 minutes. (b) FTIR spectra of freeze-dried (i) PAM-VI-50 hydrogel, (ii) the hydrogel treated with 10 mM $ZnSO_4$ + 20 mM PAG solution and (iii) hydrogel then treated with UV irradiation.

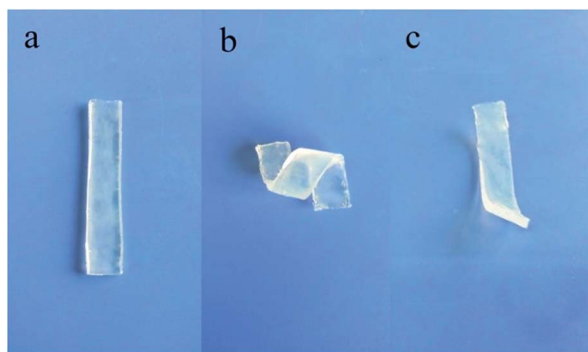


Fig. 7 Digital pictures of shape memory process of a PVA hydrogel. (a) Pristine PVA hydrogel. (b) The hydrogel was then cross-linked by borax temporarily spiral-shaped. (c) The hydrogel recovered its permanent shape after UV irradiation.

Frequency sweep (Fig. 6a) after UV irradiation demonstrates an almost identical strength of the sample in comparison with its initial state, indicating that the complexation effect is completely screened because of protonation of imidazole groups. FTIR spectroscopy has been employed in order to

further probe coordination interaction change associated with UV irradiation (Fig. 6b). On the formation of Zn^{2+} -imidazole group coordination, the indicative ring mode (R_6) peak at 915 cm^{-1} of imidazole decreases in intensity, accompanied by the formation of a new band at 954 cm^{-1} .²¹ After UV illumination, the imidazole groups become protonated and thus the peak at 954 cm^{-1} disappears.

In order to testify whether this PAG strategy is generally applicable to other conventional pre-existing shape memory hydrogels, a physical network, boronate ester cross-linked melamine-poly(vinyl alcohol) (PVA), is used. It is known that PVA and boronic acid can form pH-sensitive boronate ester.^{42,43} Therefore, it holds promise for designing a light-responsive shape memory hydrogel with a combination of the simple and practical PAG strategy.

We first introduce an additional physical network into PVA hydrogel *via* multiple hydrogen bonds with melamine according to previously reported freezing/thawing methods.⁴⁴ After cooling, the melamine-enhanced PVA hydrogel is deformed to a spiral one under external stress and treated with a mixture solution of borax and PAG (10 mM, 20 mM, respectively) to fix the temporary shape (Fig. 7). Afterwards, upon UV irradiation, the temporary shape returns to its permanent form due to the deconstruction of the boronate ester cross-linkages with hydroxyl groups from PVA. This is further proved by the drastic decrease of G' values after irradiation (Fig. S4, ESI†). Thus, the facile PAG strategy is well suitable for designing light-responsive shape memory hydrogel systems. Note that although UV is critical to construct such a shape memory hydrogel, the present strategy may be confined to those pH-sensitive systems. Application to more comprehensive systems needs to be investigated in further detail.

Conclusions

In conclusion, we propose a facile and general strategy to endow conventional hydrogels with ultraviolet (UV)-controlled shape memory performance. This convenient method is proved to be suitable for organic cross-linked poly(acrylamide-*co*-*N*-vinylimidazole) hydrogel and a melamine enhanced polyvinyl alcohol hydrogel. Photolysis of PAG generates proton, which is necessary to disassociate the additional networks that are essential for fixity of a temporary shape. Considering the difficulty for preparing light-responsive shape memory hydrogels and the simplicity of the present strategy, we believe this method undoubtedly provides a new opportunity with regard to the design and practical application of light-controlled shape memory hydrogels.

Acknowledgements

We gratefully acknowledge financial support from the National Natural Science Foundation of China (Grant no. 51273189), National Science and Technology Major Project of the Ministry of Science and Technology of China (2011ZX05010-003), Petro-China Innovation Foundation (2012D-5006-0202) and China

Postdoctoral Science Foundation funded project (no. 2013M531513).

References

- 1 D. Habault, H. Zhang and Y. Zhao, *Chem. Soc. Rev.*, 2013, **42**, 7244–7256.
- 2 K. M. Lee, H. Koerner, R. A. Vaia, T. J. Bunning and T. J. White, *Soft Matter*, 2011, **7**, 4318–4324.
- 3 J. Kunzelman, T. Chung, P. T. Mather and C. Weder, *J. Mater. Chem.*, 2008, **18**, 1082–1086.
- 4 A. Lendlein, H. Jiang, O. Junger and R. Langer, *Nature*, 2005, **434**, 879–882.
- 5 S.-Q. Wang, D. Kaneko, M. Okajima, K. Yasaki, S. Tateyama and T. Kaneko, *Angew. Chem., Int. Ed.*, 2013, **52**, 11143–11148.
- 6 T. Ikeda, M. Nakano, Y. Yu, O. Tsutsumi and A. Kanazawa, *Adv. Mater.*, 2003, **15**, 201–205.
- 7 H. Koerner, G. Price, N. A. Pearce, M. Alexander and R. A. Vaia, *Nat. Mater.*, 2004, **3**, 115–120.
- 8 H. Zhang, H. Xia and Y. Zhao, *ACS Macro Lett.*, 2014, **3**, 940–943.
- 9 S. Maity, J. R. Bochinski and L. I. Clarke, *Adv. Funct. Mater.*, 2012, **22**, 5259–5270.
- 10 H. Zhang, H. Xia and Y. Zhao, *J. Mater. Chem.*, 2012, **22**, 845–849.
- 11 Y. Wu, J. Hu, C. Zhang, J. Han, Y. Wang and B. Kumar, *J. Mater. Chem. A*, 2015, **3**, 97–100.
- 12 H. Zhang and Y. Zhao, *ACS Appl. Mater. Interfaces*, 2013, **5**, 13069–13075.
- 13 H. Zhang, J. Zhang, X. Tong, D. Ma and Y. Zhao, *Macromol. Rapid Commun.*, 2013, **34**, 1575–1579.
- 14 J. R. Kumpfer and S. J. Rowan, *J. Am. Chem. Soc.*, 2011, **133**, 12866–12874.
- 15 J. Liang, Y. Xu, Y. Huang, L. Zhang, Y. Wang, Y. Ma, F. Li, T. Guo and Y. Chen, *J. Phys. Chem. C*, 2009, **113**, 9921–9927.
- 16 E. Wang, M. S. Desai and S.-W. Lee, *Nano Lett.*, 2013, **13**, 2826–2830.
- 17 S. Thakur and N. Karak, *J. Mater. Chem. A*, 2014, **2**, 14867–14875.
- 18 A. Yasin, H. Li, Z. Lu, S. U. Rehman, M. Siddiq and H. Yang, *Soft Matter*, 2014, **10**, 972–977.
- 19 Y. Fan, W. Zhou, A. Yasin, H. Li and H. Yang, *Soft Matter*, 2015, **11**, 4218–4225.
- 20 A. Yasin, W. Zhou, H. Yang, H. Li, Y. Chen and X. Zhang, *Macromol. Rapid Commun.*, 2015, **36**, 845–851.
- 21 J. L. Lippert, J. A. Robertson, J. R. Havens and J. S. Tan, *Macromolecules*, 1985, **18**, 63–67.
- 22 M. Takafuji, S. Ide, H. Ihara and Z. Xu, *Chem. Mater.*, 2004, **16**, 1977–1983.
- 23 M. J. Molina, M. R. Gómez-Antón and I. F. Piérola, *J. Phys. Chem. B*, 2007, **111**, 12066–12074.
- 24 M. Das and E. Kumacheva, *Colloid Polym. Sci.*, 2006, **284**, 1073–1084.
- 25 B. Işık and B. Doğanterkin, *J. Appl. Polym. Sci.*, 2005, **96**, 1783–1788.
- 26 B. B. Sharma, C. Murli and S. M. Sharma, *J. Raman Spectrosc.*, 2013, **44**, 785–790.
- 27 N. Tanaka, K. Ito and H. Kitano, *Macromolecules*, 1994, **27**, 540–544.
- 28 R. J. Sundberg and R. B. Martin, *Chem. Rev.*, 1974, **74**, 471–517.
- 29 J. T. Edsall, G. Felsenfeld, D. S. Goodman and F. R. N. Gurd, *J. Am. Chem. Soc.*, 1954, **76**, 3054–3061.
- 30 L. Zhang, N. R. Brostowitz, K. A. Cavicchi and R. A. Weiss, *Macromol. React. Eng.*, 2014, **8**, 81–99.
- 31 C. W. A. Ng, M. A. Bellinger and W. J. MacKnight, *Macromolecules*, 1994, **27**, 6942–6947.
- 32 S. Schlögl, M. Reischl, V. Ribitsch and W. Kern, *Prog. Org. Coat.*, 2012, **73**, 54–61.
- 33 J. L. Dektar and N. P. Hacker, *J. Org. Chem.*, 1990, **55**, 639–647.
- 34 A. L. Fameau, A. Arnould, M. Lehmann and R. von Klitzing, *Chem. Commun.*, 2015, **51**, 2907–2910.
- 35 E. M. White, J. E. Seppala, P. M. Rushworth, B. W. Ritchie, S. Sharma and J. Locklin, *Macromolecules*, 2013, **46**, 8882–8887.
- 36 V. Javvaji, A. G. Baradwaj, G. F. Payne and S. R. Raghavan, *Langmuir*, 2011, **27**, 12591–12596.
- 37 J.-M. Raquez, S. Vanderstappen, F. Meyer, P. Verge, M. Alexandre, J.-M. Thomassin, C. Jérôme and P. Dubois, *Chem.-Eur. J.*, 2011, **17**, 10135–10143.
- 38 L. Peponi, I. Navarro-Baena, A. Sonseca, E. Gimenez, A. Marcos-Fernandez and J. M. Kenny, *Eur. Polym. J.*, 2013, **49**, 893–903.
- 39 I. Navarro-Baena, J. M. Kenny and L. Peponi, *Cellulose*, 2014, **21**, 4231–4246.
- 40 A. Saralegi, M. L. Gonzalez, A. Valea, A. Eceiza and M. A. Corcuera, *Compos. Sci. Technol.*, 2014, **92**, 27–33.
- 41 H. Chen, Y. Li, Y. Liu, T. Gong, L. Wang and S. Zhou, *Poly. Chem.*, 2014, **5**, 5168–5174.
- 42 M. Shibayama, Y. Hiroyuki, K. Hidenobu, F. Hiroshi and N. Shunji, *Polymer*, 1988, **29**, 2066–2071.
- 43 L. He, D. E. Fullenkamp, J. G. Rivera and P. B. Messersmith, *Chem. Commun.*, 2011, **47**, 7497–7499.
- 44 G. Li, Q. Yan, H. Xia and Y. Zhao, *ACS Appl. Mater. Interfaces*, 2015, **7**, 12067–12073.